Pattern Recognition Letters 126 (2019) 51–57

Contents lists available at ScienceDirect

Pattern Recognition Letters

journal homepage: www.elsevier.com/locate/patrec

3D Nose shape net for human gender and ethnicity classification ☆

Chenlei Lv, Zhongke Wu*, Dan Zhang, Xingce Wang, Mingquan Zhou

College of Information Science and Technology, Beijing Normal University, 100875, China

ARTICLE INFO

Article history:
Available online 16 November 2018

ABSTRACT

Gender and ethnicity are significant characteristics of human beings. Using human facial data to classify gender and ethnicity of people is important in facial analysis research. A novel method is proposed to address this issue. The method is based on a 3D nose shape organization structure called "3D nose shape net". To construct the 3D nose shape net, a nose measurement method to determine the distances between different noses and to use the results to cluster noses is proposed. Using the nose clustering results, the 3D nose shape net is constructed. The proposed method uses only the nose data from the 3D face; it is robust to facial expressions and facilitates removal of the poses effect. The 3D nose shape net does not consider the texture information in the nose region; therefore it is robust to illumination and cosmetics on faces. Gender and ethnicity classification results are achieved in 3D nose shape net simultaneously. The experimental 3D nose shape nets are built and tested using the FRGC2.0 and Bosphorus3D datasets.

1. Introduction

Gender and ethnicity classification tasks are important in facial analysis works. In many applications such as face recognition, medical research, and anthropology studies, automatic gender and ethnicity classification provide necessary pre-process results for precise statistical analysis. In most cases, humans can estimate gender and ethnicity characteristics from human faces by vision directly. However, the estimate process by human vision is limited by some factors such as hair style, head poses, facial expressions, illumination, and cosmetics. In 2D facial images, such factors are difficult to remove. In recent years, 3D scanning equipment is becoming more popular and is being used in many applications, and constructing a gender and ethnicity classification framework in 3D facial data is now feasible. Our method for gender and ethnicity classification is based on 3D noses of 3D facial data. Using 3D noses in classification tasks has several advantages: nose shape is robust to facial expressions and is essentially unaffected by hair; the nose region is robust to facial expressions; noses from people with different gender and ethnicity characteristics have obvious differences, and are convenient to study.

In this paper, we study the differences of noses from people with different gender and ethnicity characteristics. We build a 3D nose shape net to achieve the goal. Constructing the 3D nose shape net consists of three main steps: 1:Pre-processing the 3D nose region — the pre-process includes 3D facial landmarks detection and face cropping. 2:Nose similarity measure — we extract certain curves from the nose and map the curves in curve shape space to measure curves distance in the shape space which can be used to measure nose similarity. 3:3D nose shape net construction — we construct a nose similarity measure matrix from a facial database and use the matrix to cluster different noses. The 3D nose shape net is constructed based on the nose clustering results. In Fig. 1, we show the flow process of the framework. In summary, our main contributions are as follows:

1) We propose a 3D nose shape net which organizes different nose shapes in a hierarchical structure. Through the 3D nose shape net, the gender and ethnicity classification results can be achieved at the same time. The classification process in the net is based on simple statistical analysis of nose shapes, and does not require complex learning algorithms.
2) We propose a nose similarity measurement method. The measurement method is based on the curves measurement in the curve shape space. The measurement in the curve shape space is not affected by 3D coordinates or the length of curves. Therefore, the nose similarity measure method is not affected by the curve representation in 3D space, and thus has more accurate measurement results.
3) We propose an automatic pipeline to construct the 3D nose shape net. It includes pre-processing of 3D nose data, nose similarity measurement, and nose clustering. The pipeline is focused on 3D nose shape analysis; it reduces the difficulty of

☆ **Conflict of interest.** The authors declare no conflict of interest.

* Corresponding author.
E-mail address: zwu@bnu.edu.cn (Z. Wu).

https://doi.org/10.1016/j.patrec.2018.11.010
0167-8655/

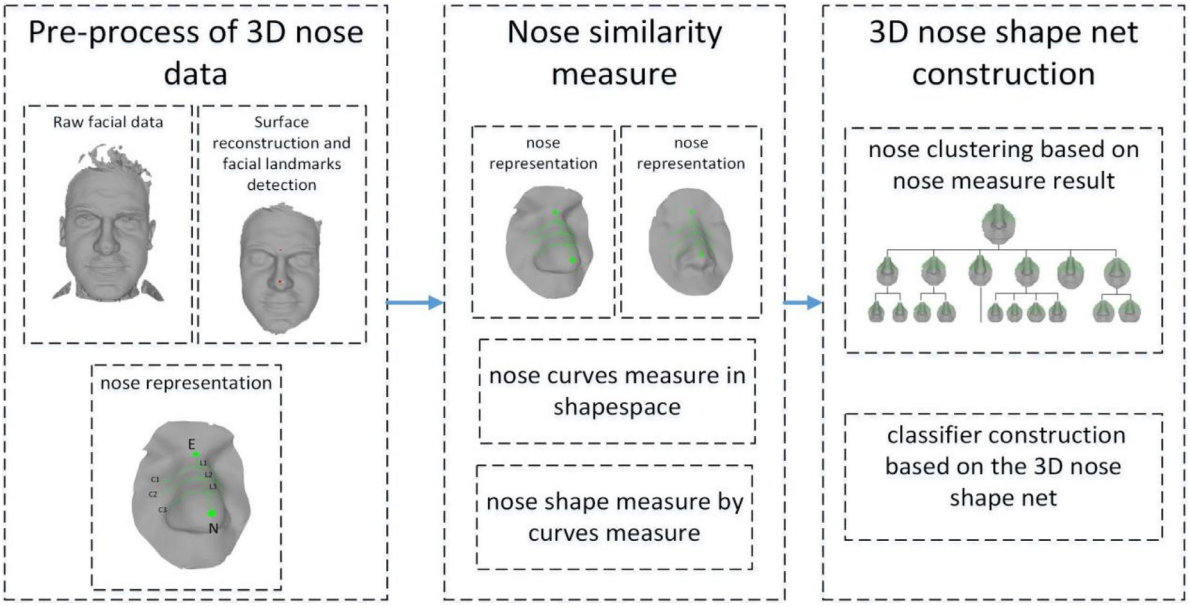

Fig. 1. The pipeline for constructing the 3D nose shape net.

mesh reconstruction and repair. The nose shape is robust to facial expressions and is not affected by hair.

The remaining parts of the paper are organized as follows. In Section 2, we present related work on facial classification and nose analysis. In Section 3, we illustrate the pre-processing of 3D nose data. In Section 4, we propose the nose similarity measure method. In Section 5, we show the 3D nose shape net construction and classification method in the net. In Section 6, we use our method on the public facial databases FRGC2.0 and Bosphorus3D for experiment.

2. Related work

With the development of face recognition technology, the research into automatic facial data classification has become more popular and significant. Basically, the related work can be divided into three categories: 2D image-based, multi-modal facial data-based, and 3D geometric feature-based.

2D image based approaches build the gender or ethnicity classification framework from facial images. Most work used machine learning technologies to build classifiers such as the Support Vector Machine (SVM) [1,4,5 and 9], Linear Discriminant Analysis (LDA) [3], Principal Component Analysis (PCA) [8], and the convolutional neural network (CNN) [10]. The facial features included binary rectangle features [2], facial landmarks [5,7], Biologically-Inspired Features [8], demographic informative features [9], the Gabor filter process features [5,6] and the special curves [23]. The features are based on pixels in facial images. There are several influencing factors that limit classification — illumination conditions, hair occlusion, head poses, and facial expressions. Such factors are difficult to remove at the pixel level. Therefore, such methods require high quality input facial images to achieve precise classification results.

Multi-modal facial data based approaches combine facial texture and shape information to establish gender or ethnicity classifier. Some works focused on image features such as Local binary pattern (LBP) [12,13 and 15] and local circular patterns (LCP) [14]. The algorithms require supplemental 3D facial data. The classical learning frameworks were used to build classifiers, such as Principal Geodesic Analysis (PGA) [11], random forest [13], AdaBoost [14], and PCA [15]. Wu [11] proposed a gender classification method based on 2.5D facial needle maps. The method focused on facial shape modeling. The texture was used as auxiliary information. The Multi-modal facial data based approaches considered 2D texture and 3D shape in facial classifiers. The features were extracted by Multi-modal facial data analysis. The methods were more robust than 2D image based approaches; however, efficient integration of 2D and 3D information for classification purposes was difficult to achieve. The classification scheme depended on the Multi-modal features, where features were extracted from single mode and other auxiliary information. The classification performance was limited by the Multi-modal features and the fusion algorithm employed.

3D geometric feature based methods focus on facial geometric information analysis. Common classifier methods are SVM [16,17], Adaboost [18], LDA [20], PCA [22], and Random Forest [19]. Han [16] built geometric features from different 3D facial regions. Hu et al. [17] extracted 3D facial shapes based on profiles and curvature. Gilani et al. [20] selected 3D facial landmarks and geodesic distances as gender features. Xia proposed a gender classification method based on 3D Facial Symmetry analysis [19]. He also combined averaged face information for gender classification [21], and extended the methods to gender facial classification tasks [25]. The advantages of the methods are based on 3D geometric feature analysis. The 3D geometric features are robust to texture noise. However, it was difficult to achieve a high quality triangular mesh from raw facial scanning data and the 3D geometric features were limited by the automatic face cropping technology. Some influencing factors such as hair, beard, and facial expressions were difficult to remove.

In summary, such methods were limited by the raw facial data in different levels. Therefore, we focus on the 3D nose region rather than the entire face to build gender and ethnicity classification. It is convenient to construct a triangular mesh form based on the nose region. The reason is the geometric information in nose region is relatively stable for different facial expressions and hair occlusion has little influence on the raw data in the nose region. The effectiveness of the nose shape has been highlighted in some facial data analysis research [24,26 and 27]. In the following sections, we discuss our nose shape analysis framework for gender and ethnicity classification.

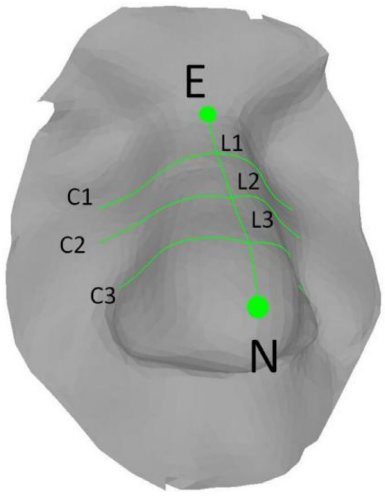

Fig. 2. Nose curves on a 3D nose region.

3. Pre-processing for 3D nose

The first step in our method is to achieve high quality 3D nose shape representation with certain facial landmarks. Therefore, we propose pre-processing of 3D noses from 3D facial data. The process includes facial surface reconstruction from the raw data, facial landmarks detection and nose shape construction. For facial surface reconstruction and facial landmarks detection, we apply two methods; a ball pivoting algorithm [28] and a shape regression algorithm [29]. Through the two methods, the 3D facial surface with landmarks is constructed. Next, we are focus on nose shape construction.

The nose shape construction phase includes two steps; nose region division and nose curves extraction. Using nasal tip landmarks, we divide the nose region of the 3D facial surface using an iso-geodesic circle. We first compute the geodesic path G_l between nasal tip and the center of the eyebrows. Next, we compute geodesic distances from all vertexes to the nasal tip and select the vertexes which have shorter geodesic distances than distance G_l. Finally, we remove other vertexes and define the nose region. The nose region meshes from different 3D facial data are aligned by nasal tip and geodesic distance G_l.

To develop nose shape features for accurate analysis, we propose an appropriate nose representation. The nose representation should satisfy several requirements: 1. the representation saves the main geometric information of the 3D nose; 2. the representation should have regular form for each nose; 3. the representation should not be too complex. On the basic of the above considerations, we extract several curves from the 3D nose region to construct nose shapes which we call “nose curves”. The nose curves are chosen from the nose area that has obvious geometric features, and the curves represent the shape of the nose in a direct manner. The definition of nose curves is a set of geodesic curves that are orthogonal to the bridge of the nose. One end point of the nose curve is in the geodesic path G_l, and the other is in the geodesic circle that has a certain geodesic distance to the nasal tip. The nose curves thus represent the geometric features of the nose region. Fig. 2 indicates the pattern of nose curves evaluated, and (3.1) is the mathematical representation of the process.

In (3.1), N_c represents the set of nose curves. Nb is the bridge of the nose (equal to G_l) and l is the point on Nb. $G(c,\ l)$ is the geodesic curve in the facial surface with two end points c and l. Additionally, c is the point in the geodesic circle S that has a certain geodesic distance (the length of G_l) to the nasal tip. The tangent vector of the geodesic path $G(c,\ l)$ is perpendicular to the tangent vector of Nb at point l. By default, the specific geodesic distance is the geodesic distance between the nasal tip and the center of the eyebrows. The surface of the nose region is constructed by the N_c. In Fig. 2, we show the instances of several nose curves in the 3D facial surface. N is the nasal tip, E is the center of the eyebrows, and $Nb = G(E, N)$, the distance of Nb, is equal to $N_c = \{G(C1, L1), G(C2, L2), G(C3, L3)\}$. The nose shape is represented by N_c.

$$N_c = \{G(c,l)|l \in Nb, c \in S, T\{G(c,l)\} \perp T\{Nb\}(l)\} \tag{3.1}$$

4. Nose similarity measure

The nose curve set represents the 3D nose shape. In this part, we propose the nose similarity measure method based on nose curves. Kendall [30] proposed shape space theory for curves measurement previously. The shape space is a quotient space of isometric Lie-group actions. Different transformations such as scaling, translation, and rotation are Lie groups that act smoothly on a manifold. The Lie group actions have been removed from the shape space.

$$M/G = \{[p]|p \in M\} \tag{4.1}$$

In (4.1), G is a Lie group that is acting smoothly on a manifold M. For p in M, the orbit of p is defined as $[p]$. In our measurement method, shape space theory is used to build the nose curves shape space for nose similarity measurements. The nose curves shape space can be regarded as M/G and the nose curve can be regarded as p. The measurement between curves is defined by the geodesic distance in the space. The nose measurement result can be achieved by the sum of the curves measurement. In (4.2), we show the nose measurement between two noses.

$$d(N_1, N_2) = \int_{Nb} G_s(C1_l, C2_l) d(l) \tag{4.2}$$

N_1 and N_2 are two noses, which are represented by nose curve sets $C1$ and $C2$, respectively. G_s is the measurement between two nose curves in the curves shape space. For the discrete case, the nose measurement is shown in (4.3). Here, g is the number of nose curves for one nose.

$$d(N_1, N_2) = \sum_{l=1}^{g} G_s(C1_l, C2_l) \tag{4.3}$$

To obtain the measurement of different noses, we should provide the function G_s. G_s is the geodesic distance between two nose curves in shape space. The computation process of G_s requires two steps: mapping nose curves into the shape space and geodesic distance computation. To map the curves into the shape space, we propose a regular curve representation. The representation is a discrete form which is shown in (4.4).

$$C_v = \{v_1, ..., v_k\}, C_v(t) = v_t, v_t \in C_v \tag{4.4}$$

C_v is the arc length parameterization of the nose curve, and it includes a set of vectors to represent the curve, where v is a vector in C_v, which is defined by two points in the curve. Here, k is the number of points in the nose curve. In practice, k is a certain constant that changes the continuity problem to a discrete problem. In (4.5), we normalize the vectors in C_v. The vectors in C_v are represented by a direction vector multiplied by a specific step length. The direction vector can be achieved by the original vector's unitization. The specific value is the reciprocal of k. The representation is invariant to scaling and translation.

$$\begin{aligned} C_v' &= \{v_1', ..., v_k'\} \\ v_t' &= v_t/(k \cdot \|v_t\|) \\ &\sum_{t=1}^{k} \left\|v_t'\right\| = 1 \end{aligned} \tag{4.5}$$

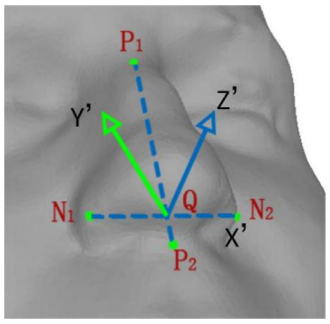

Fig. 3. The local coordinate system (X′, Y′, Z′). P_1, P_2, N_1 and N_2 are certain facial landmarks whose positions are relatively robust to facial expressions. First, we compute Z′ by the cross product of vectors $\overrightarrow{P_2P_1}$ and $\overrightarrow{N_2N_1}$. The point Q is in the $\overrightarrow{N_2N_1}$. X′ is $\overrightarrow{N_2Q}$. Y′ is the cross product of X′ and Z′.

The vectors in C' are transformed to the local coordinate system (Fig. 3) by T in (4.6). Using the new vector representation, we achieve the geodesic distance between the two curves in shape space using (4.7). By combining (4.3) and (4.7), we determine the nose similarity measure result.

$$C_v' = \{T(v_1'), ..., T(v_k')\} \tag{4.6}$$

$$G_s(C_1, C_2) = \arccos\langle C_1, C_2\rangle \tag{4.7}$$

5. 3D nose shape net construction

Using the nose similarity measurement method, we can construct a nose similarity matrix from a facial database. Based on the nose similarity matrix, we propose the 3D nose shape net (3DNSN). The 3DNSN represents an organized framework of 3D noses. Different noses in 3DNSN are divided into different classes by the nose similarity measure matrix. Using a clustering method, we can determine the different nose classes. The 3DNSN includes nose similarity information with different shapes. To build a gender and ethnicity classifier, we propose an estimation function based on the 3DNSN. In the following paragraphs, we discuss the 3DNSN construction and estimation function.

3DNSN construction is based on the nose similarity matrix. The clustering features are similarity values between different noses. The similarity value can be regarded as the "distance" between noses. We use the classical clustering method, Affinity Propagation (AP), to determine different classes from the nose similarity matrix. The AP method clusters data based on distance information. The method is not limited by the dimension space because it adapts the characteristics of the nose similarity matrix. We use the nose similarity matrix as the input data in AP. Finally, we construct the 3DNSN with a two-level nose structure.

For statistical computation, we propose the mean nasal shape defined in (5.1) and (5.2), which can be regarded as the center nose of a nose class. S represents the nose class in 3DNSN. For a randomly selected nose N_m in the nose class, the function $V(N_m)$ is the sum of the distance between nose N_m and other noses N_i in S. The mean nasal shape of S is the nose with the minimum value of V.

$$S = \{N_1, ...N_n\}, V(N_m) = \sum_{i=1}^{n} d(N_m, N_i) \tag{5.1}$$

$$\overline{N} = \arg\min_{N_m \in S} V(N_m) \tag{5.2}$$

Our estimation function is based on the 3DNSN. The basic hypothesis of estimation function construction is that the nose shape is consistent with gender and ethnicity characteristics. When different noses have similar shape features, they have higher probability of sharing the same gender and ethnicity characteristics. The ideal solution of the classifier is inputting the source nose shape into the 3DNSN and searching the target nose shape for the class with the most similar shape features. The gender and ethnicity of the target nose are based on the classification result of the source nose. However, the solution is limited by the scale of 3DNSN. The classification result of 3DNSN is not accurate when the 3DNSN does not include a similar nose shape to the source. To solve the problem, we should consider more nose data in 3DNSN construction and combine several similarity measurements in 3DNSN to achieve better classification results. In (5.3), we show the estimation function C based on 3DNSN.

Algorithm 1 Estimation function C_{gender}.

```
1: Input N_s.
2: for i = 1 to n //n is the number of classes in 3DNSN
3:    add d (N_s, N_i) to list //N_i is the mean nose in class i.
4: end for //the list can be regard as the index of the class of 3DNSN.
5: sort(list)
6: for i = 1 to k from list
7:    achieve the N_male from male nose data in list i
8:    achieve the N_female from female nose data in list i
9:    achieve p_female by N_male, N_female, N_s
10: put p_female into list(p)
11:end for
12: for i = 1 to k from list
13:    achieve w_i from N_s, N_i
14:    put w_i into list(w)
15: end for
16: C_gender is achieved by list(p) and list(w).
```

$$C_{gender/ethnicity}(N_s) = \sum_{i=1}^{k} w_i * p_{i(gender/ethnicity)}(N_s) \tag{5.3}$$

$$w_j = \frac{\pi - d(N_s, N_j)}{\sum_{i=1}^{k} d(N_s, N_i)}, j \in [0, k] \tag{5.4}$$

$$p_{female}(N_s) = 1 - \left(\frac{\min(d(N_s, N_{female}))}{\min(d(N_s, N_{male})) + \min(d(N_s, N_{female}))}\right) \tag{5.5}$$

$$p_{Asia}(N_s) = 1 - \left(\frac{\min(d(N_s, N_{Aisa}))}{\min(d(N_s, N_{Asia})) + \min(d(N_s, N_{other}))}\right) \tag{5.6}$$

N_s is the source nose. k is the number of classes we select in 3DNSN. It is less than the sum of all classes in 3DNSN. In (5.4), w is the weight of each clustering center in the estimation function, and is dependent on k. The value of w is computed by the similarity measure from N_s to each mean nose in the class. In (5.5), the probability function p is computed in the class of 3DNSN. In certain classification problems, we achieve the most similar nose with certain classification characteristics and compute the rate with the most similar nose with other classification characteristics. For instance, we want to achieve the probability that the nose comes from a female. We evaluate the most similar nose N_{female} to N_s from female nose data. We also achieve the most similar nose N_{male} to N_s from male nose data. We compute the rate of the distances ratio. The distance d is inversely proportional to the probability p, therefore we subtract the distances ratio from 1 to achieve the probability p. The ethnicity estimation is similar to the gender classification, as shown in (5.6). Algorithm 1 outlines the procedure to compute the gender classification estimation function C_{gender}.

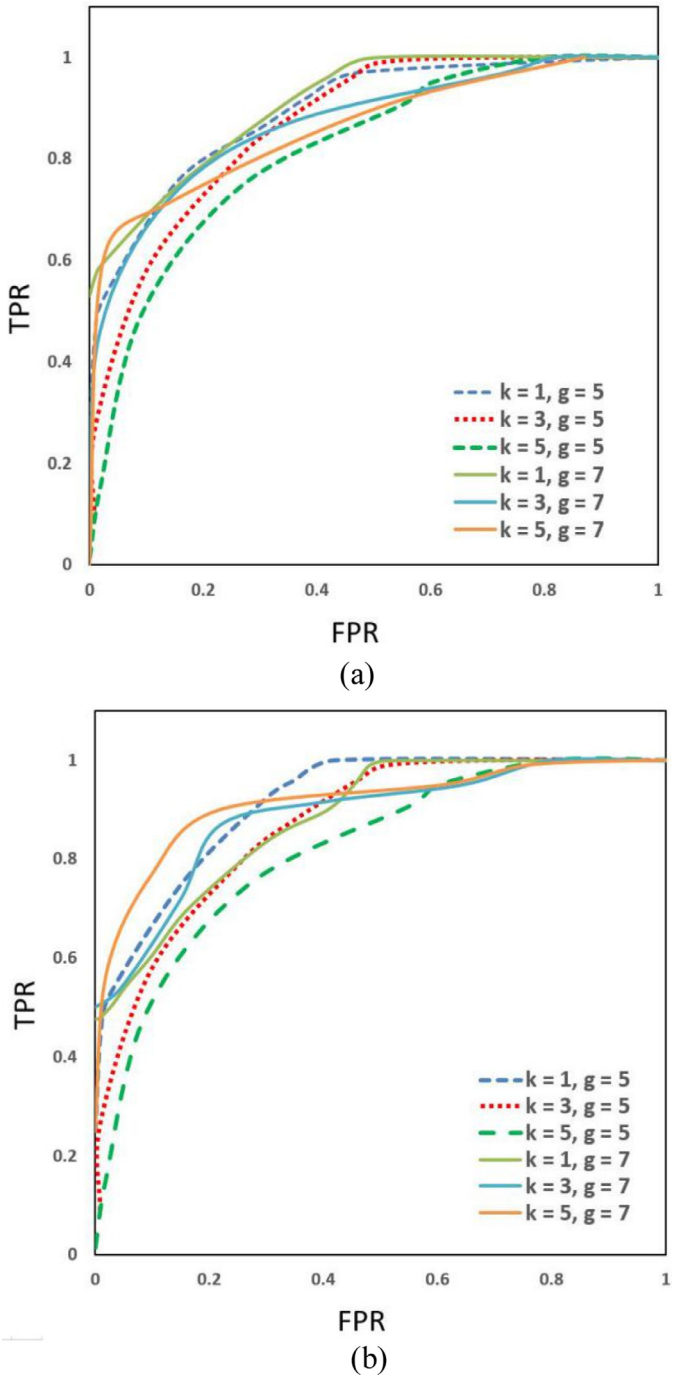

Fig. 4. The ROC results of facial classification with different parameters ($k = \{1, 3, 5\}$, $g = \{5, 7\}$). (a) is the gender classification result (for male). (b) is the ethnicity classification result (for white).

6. Experiments

In the following experiments, we build the 3DNSN from the facial databases FRGC2.0 and Bosphorus3D. The 3D facial database FRGC2.0 has been widely used in face recognition and facial classification. It includes three subsets: Fall2003, Spring2003, and Spring2004. Totally, FRGC2.0 includes about 4,000 3D face scans from 466 people, 1,848 scans of 203 females and 2,159 scans of 265 males. The facial data samples for each person have different facial expressions. The 3D facial database Bosphorus3D includes 4666 facial data from 105 persons. The facial data in Bosphorus3D have different expressions, head poses, glasses and hair occlusion. Regarding ethnicity, most samples belong to White and Asian classes. There are few samples of black and hybrid ethnicities. To estimate gender and ethnicity classification performance of the 3DNSN, we use three steps for illustration. First we discuss some parameters that influence 3DNSN construction. Second, we select different training sets from FRGC2.0 to estimate the data sensitivity of 3DNSN. Finally, we compare the classification performance of several methods and summarize the results. For classifier evaluation in FRGC2.0, we use the subset (Fall2003, 1829 samples) of FRGC2.0 to build the 3DNSN and other samples (2264 samples) to be the test set. For classifier evaluation in Bosphorus3D, we use 630 samples (6*105) to build the 3DNSN and other samples to be the test set. Some samples in Bosphorus3D have different head poses and hair occlusion. The nose shape can't be represented by the whole nose region. We extract the nose curves from half face from the samples.

Table 1
Gender classification rate in different ethnicity groups.

Ethnicity group	Group1(Asian)	Group2(White)
female	84.25%	89.95%
male	78.75%	85.28%

Table 2
Ethnicity classification rate in different gender groups.

Gender group	Group1(female)	Group2(male)
Asian	95.85%	82.32%
White	92.54%	94.45%

6.1. Parameters that influence estimation

In 3DNSN, the parameter configuration decides the classification performance. Specifically, the key parameters are the nose curves number g in (4.3) and the class number k in (5.3). The nose curves number g represents the precision of the nose shape representation. It decides the balance between nose measurement speed and accuracy. When g is too large or too small, the balance will be broken, and the nose similarity measurement process will become unstable. Parameter k influences the accuracy of classification in 3DNSN. The 3DNSN includes dozens of subclasses in the first level, where each subclass represents one type of nose shape from the nose data set. Parameter k decides the range of nose shapes to be used in the classification process. The proper value of k provides the balance between computation speed and classification accuracy. We select 810 samples from 240 people from FRGC2.0 randomly for test purposes.

In Fig. 4, the ROC results show two fundamental conclusions. First, the ethnicity classification results are better than the gender classification results on average. The differences between nose shapes from different ethnicity groups facilitate recognition of ethnicity relatively easily. Secondly, different parameter configurations affect the classification results without linear limits in a certain range. We think the reason is that the quality of the 3D scanning data is different. Nose shapes with different accuracies influence the stability of the classification process. When the parameters are out of range, the classification results of 3DNSN become unstable ($k > 7$, $g > 7$). In the following experiments, we use the parameter configuration ($k = 3$, $g = 5$) as this combination displays relatively stable classification performance.

Table 3
Gender classification rate in different groups.

Ethnicity group	Group1(Asian female and White male)	Group2(Asian male and White female)
female	94.25%	89.95%
male	98.75%	85.28%

Table 4
Ethnicity classification rate in different groups.

Gender group	Group1(Asian female and White male)	Group2(Asian male and White female)
Asian	98.85%	80.13%
White	99.54%	82.31%

Table 5
Comparison of our method to earlier methods in FRGC2.0.

Method	Object	Database	Gender Classification Rate			Ethnicity Classification Rate		
			Female	Male	Average	Asian	White	Average
Ballihi 2012	3D face	FRGC2.0	–	–	84.98%	–	–	–
Xia 2013	3D + 2D face	FRGC2.0	–	–	93.27 ± 5%	–	–	–
Huang 2014	3D + 2D face	FRGC2.0	94.91%	95.96%	95.50%	99.13%	99.90%	99.45%
Gilani 2013	3D face	FRGC2.0	–	–	97.05%	–	–	–
Xia 2015	3D face	FRGC2.0	–	–	92.4 ± 3.58%	–	–	–
Xia 2017	3D face	FRGC2.0	–	–	93.61%	–	–	96.60%
Our method	3D nose	FRGC2.0	87.4%	92.3%	89.4%	89.2%	97.4%	93.3%

Table 6
Comparison of our method to earlier methods in Bosphorus3D.

Method	Object	Database	Gender Classification Rate			Ethnicity Classification Rate		
			Female	Male	Average	Asian	White	Average
Huang 2014	3D face	Bosphorus3D	84.9%	87.9%	86.5%	84.1%	90.9%	87.4%
Xia 2017	3D face	Bosphorus3D	83.3%	87.2%	85.6%	88.1%	92.4%	90.2%
Our method	3D nose	Bosphorus3D	89.2%	92.3%	91.2%	89.2%	97.4%	93.3%

6.2. Data sensitive estimation

In our framework, we process the gender and ethnicity classification tasks simultaneously. We use the same test set which has been introduced in Section 6.2. The gender and ethnicity characteristics influence each other's classification results. For example, the gender classification results are not same for Asian and White groups by nose shape analysis. The reason is that nose samples from different gender and ethnicity groups have different degrees of similarity. In Tables 1 and 2, we show different classification results from the samples with different gender and ethnicity characteristics in FRGC2.0.

From Tables 1 and 2, we arrive at two basic conclusions regarding classification tasks. First, the ethnicity classification results are better than the gender classification results using nose shape analysis. Second, the accuracy of gender classification results is different for people with different ethnicity characteristics. Different ethnic groups have different nose clustering characteristics. The ethnicity classification results of Asian females and White males are much better. However, in gender classification, the Asian females and White males do not achieve better results. In summary, the data suggests that Asian females and White males have lower values of nose similarity in their respective groups. In Tables 3 and 4, we show comparisons of classification results from different groups in FRGC2.0. The results show that the classification results become much better when the Asian female and White male groups are removed.

6.3. Comparison and summary

In Table 5, we show the comparison between our method and other methods in FRGC2.0. Some methods focus on single classification problems. Several methods process the gender and ethnicity classification simultaneously. For a large database such as FRGC2.0, the classification accuracy of our method is close to [27], which is similar to our method. However, the classification results of our method are worse than the methods which are based on multimodal facial data and accurate geometric analysis models on average. Our classification process is based on nose similarity measurement results in 3DNSN. We do not use a classical machine learning framework to build the classifier. The classification accuracy is affected by the nose samples discussed in Section 6.2. The advantages of our method is robust to different facial expressions, head poses and some occlusions (hair and glasses). In Table 6, we compare the classification rate of several methods in Bosphorus3D. Actually, the methods based on the whole facial data are influenced by the facial expressions, head poses, hair and glasses obviously. Some samples in Bosphorus3D are influenced by different head poses, glasses and hair occlusions. The complete surface can't be achieved. One side of the facial data is unclear. We extract the nose curves from half face with clear features of the samples. The facial data is symmetrically. The nose curves from half face can be used to represent the nose shape in a certain extent.

In summary, the gender and ethnicity classification process based on nose shape analysis is feasible. The method can achieve similar classification rates to other methods which are based on global facial data. Our method classification results will vary depending on the nose similarity measurements available in a dataset. In certain data sets, the classification rate of our method can achieve the best results. However, our method is limited by several factors; first, the representation of the nose data. In Section 6.1, we show the influence of parameter g with different values; second, the facial data from different groups in 3DNSN con-

Table 7
Gender classification rate based on nose samples.

Nose number in 3DNSN	Gender classification in average	Ethnicity classification in average
50	62.3%	66.52%
100	72.35%	78.44%
200	86.3	92.3%

struction. The classification rate of our method depends on the diversity of the nose shapes in 3DNSN. If the facial data are not sufficient in number, or are not diverse enough for effective 3DNSN construction, the classification results are poor and classification may become unstable. To show the influence of this factor, we compare the classification results with different numbers of nose data in 3DNSN construction (Table 7). The classification rate is in inverse proportion to the scale of the nose number in 3DNSN.

7. Conclusion

We proposed a gender and ethnicity classification method by constructing a 3DNSN. The method is based on nose similarity measurement. The nose similarity measurement is achieved by the combination of the nose's curve distances, which are computed in the curve shape space. Using nose data in classification has many advantages; nose data are relatively robust to facial expressions; occlusions caused by hair, eyebrows, and beards hair have little influence on the nose region; the 3D facial surface in nose region is smoother. In experiments, we show the classification results and demonstrate that the results of 3DNSN are similar to classical methods based on global facial data. However, our classification method is affected by the number of noses included in the 3DNSN. In nose similarity measurements, the nose shape is considered as a set of nose curves. The measurement is a simple linear combination of curve distances, which causes the global features of the entire surface of nose region to be lost. In future work, we will collect more nose shapes in a larger database to evaluate optimal parameters for 3DNSN construction, and to improve nose similarity measurement, we will evaluate effective computational methods to determine global measurement of the nose region.

Acknowledgments

This work is partially supported by the National Key Research and Develop Program of China (no. 2017YFE0100500, no. 2017YFB1002600), the Chinese High-Technical Research Development Foundation Program (no. 2015AA020506), Beijing Natural Science Foundation of China (no. 4172033). We thank the face databases (FRGCv2.0 and Bosphorus3D) and method's code provider in Github.

References

[1] B. Moghaddam, M.H. Yang, Gender classification with support vector machines, in: IEEE International Conference on Automatic Face and Gesture Recognition, 2000, p. 306.
[2] G. Shakhnarovich, P.A. Viola, B. Moghaddam, A unified learning framework for real time face detection and classification, in: IEEE International Conference on Automatic Face and Gesture Recognition, 2002, pp. 14–21.
[3] X. Lu, A.K. Jain, Ethnicity identification from face images, in: SPIE International Symposium on Defense and Security: Biometric Technology for Human Identification, 2004, pp. 114–123.
[4] S. Hosoi, E. Takikawa, M. Kawade, Ethnicity estimation with facial images, in: IEEE International Conference on Automatic Face and Gesture Recognition, 2004, pp. 195–200.
[5] H.C. Lian, B.L. Lu, E. Talikawa, S. Hosoi, Gender recognition using a min-max modular support vector machine, in: International Conference on Natural Computation, 2005, pp. 438–441.
[6] H. Lu, H. Lin, Gender recognition using adaboosted feature, in: IEEE International Conference on Natural Computation, 2007, pp. 646–650.
[7] A. Samal, V. Subramani, D. Marx, Analysis of sexual dimorphism in human face, J. Vis. Commun. Image Represent. 18 (6) (2007) 453–463.
[8] G. Guo, G. Mu., A study of large-scale ethnicity estimation with gender and age variations, in: IEEE Computer Society Conference on Computer Vision and Pattern Recognition Workshops, 2010, pp. 79–86.
[9] H. Han, C. Otto, X. Liu, A. Jain, Demographic estimation from face images: human vs. machine performance, IEEE Trans. Pattern Anal. Mach. Intell. 37 (6) (2015) 1148–1161.
[10] S.L. Shan, M. Khalil-Hani, S.A. Radzi, R. Bakhteri, Gender classification: a convolutional neural network approach, Turk. J. Electric. Eng. Comput. Sci. 24 (3) (2016) 1248–1264.
[11] J. Wu, W. Smith, E.R. Hancock, Gender classification using shape from shading, in: British Machine Vision Conference September, 2007, 2007, pp. 1039–1048.
[12] G. Zhang, Y. Wang, Multimodal 2D and 3D facial ethnicity classification, in: Fifth International Conference on Image and Graphics, IEEE Computer Society, 2009, pp. 928–932.
[13] B. Xia, B.B. Amor, D. Huang, et al., Enhancing gender classification by combining 3D and 2D face modalities, in: Signal Processing Conference, IEEE, 2013, pp. 1–5.
[14] D. Huang, H. Ding, C. Wang, et al., Local circular patterns for multi-modal facial gender and ethnicity classification, Image Vision Comput. 32 (12) (2014) 1181–1193.
[15] A Moeini, H. Moeini, Pose-invariant gender classification based on 3D face reconstruction and synthesis from single 2D image, Electron. Lett. 51 (10) (2015) 760–762.
[16] X. Han, H. Ugail, I. Palmer, Gender classification based on 3D face geometry features using SVM, in: International Conference on Cyberworlds, IEEE Computer Society, 2009, pp. 114–118.
[17] Y. Hu, J. Yan, P. Shi, A fusion-based method for 3D facial gender classification, in: International Conference on Computer and Automation, Engineering, 2010, pp. 369–372.
[18] L. Ballihi, B.B. Amor, M. Daoudi, A Srivastava, D Aboutajdine, Geometric based 3D facial gender classification, in: International Symposium on Communications Control and Signal Processing, IEEE, 2012, pp. 1–5.
[19] B. Xia, B.B. Amor, H. Drira, et al., Gender and 3D facial symmetry: what's the relationship? in: IEEE International Conference and Workshops on Automatic Face and Gesture Recognition, IEEE, 2013, pp. 1–6.
[20] S.Z. Gilani, F. Shafait, A.S. Mian, Biologically significant facial landmarks: how significant are they for gender classification? in: International Conference on Digital Image Computing: Techniques and Applications, 2013, pp. 1–8.
[21] B. Xia, B.B. Amor, H. Drira, M. Daoudi, L. Ballihi, Combining face averageness and symmetry for 3D-based gender classification, Pattern Recognit. 48 (3) (2015) 746–758.
[22] R. Tokola, A. Mikkilineni, C. Boehnen, 3D face analysis for demographic biometrics, in: International Conference on Biometrics, IEEE, 2015, pp. 201–207.
[23] Y Wang, C. Chen, M Albert, et al., Eyebrow shape analysis by using a modified functional curve procrustes distance, in: IEEE Sixth International Conference on Biometrics: Theory, Applications and Systems, IEEE, 2013, pp. 1–7.
[24] M Emambakhsh, A.N. Evans, M Smith, Using nasal curves matching for expression robust 3D nose recognition, in: IEEE Sixth International Conference on Biometrics: Theory, Applications and Systems, IEEE, 2013, pp. 1–8.
[25] B. Xia, B.B. Amor, M. Daoudi, Joint gender, ethnicity and age estimation from 3D faces: an experimental illustration of their correlations, Image Vision Comput. 64 (2017) 90–102.
[26] H. Drira, B. Amor, A. Srivastava, M. Daoudi, A Riemannian analysis of 3D nose shapes for partial human biometrics, IEEE International Conference on Computer Vision. September, 2009, doi:10.1109/ICCV.2009.5459451.
[27] M. Emambakhsh, A.N. Evans, Nasal patches and curves for an expression-robust 3D face recognition, IEEE Trans. Pattern Anal. Mach. Intell. 39 (5) (2016) 995–1007.
[28] F. Bernardini, J. Mittleman, H. Rushmeier, et al., The ball-pivoting algorithm for surface reconstruction, in: Visualization & Computer Graphics IEEE Transactions on, 5, 1999, pp. 349–359.
[29] F.M. Sukno, J.L. Waddington, P.F. Whelan, 3-D facial landmark localization with asymmetry patterns and shape regression from incomplete local features, IEEE Trans. Cybern. 45 (9) (2015) 1717.
[30] D.G. Kendall, Shape manifolds, procrustean metrics, and complex projective spaces, Bull. Lond. Math. Soc. 16 (2) (1984) 81–121.